PROCEEDINGS OF SCIENCE

Recent Dark Matter related searches with the *BABAR* detector.

Hossain Ahmed[a,b,*] **and Nafisa Tasneem**[a] **on behalf of the** *BABAR* **collaboration**

[a] *St. Francis Xavier University, 4130 University Avenue, Antigonish, Nova Scotia, Canada*

[b] *Department of Physics and Astronomy, University of Victoria, Elliot Building, Victoria, British Columbia, Canada*

E-mail: hahmed@stfx.ca

We present the most recent *BABAR* searches for reactions that could simultaneously explain the presence of dark matter and the matter-antimatter asymmetry in the universe. This scenario predicts B-meson decays into an ordinary-matter baryon and a dark-sector anti-baryon ψ_D with branching fractions accessible at the B factories. The results are based on the full data set of about 430fb^{-1} collected at the Υ(4S) resonance by the *BABAR* detector at the PEP-II collider. We search in particular, for decays like $B^0 \rightarrow \psi_D \mathcal{B}$, where $\mathcal{B}$ is a Standard Model (SM) baryon (proton, Λ, or Λ_c). The hadronic recoil method has been applied with one of the B mesons from Υ(4S) decay fully reconstructed, while only one baryon is present in the signal B-meson side. The missing mass of signal B meson is considered as the mass of the dark particle ψ_D. Stringent upper limits on the decay branching fraction are derived for ψ_D masses between 1.0 and 4.2 GeV/c^2.

The European Physical Society Conference on High Energy Physics (EPS-HEP2023)
21-25 August 2023
Hamburg, Germany

[*] Speaker

https://pos.sissa.it/

PoS(EPS-HEP2023)048

1. Introduction

The evidence for the existence of dark matter (DM) is evident from astrophysical observations, i.e., the precision measurements of cosmic microwave background (CMB) by the Planck satellite [1,2]. The matter dominance in the universe, on the other hand, is also a pressing issue in modern particle physics as our known cosmology indicates an early hot universe born with an equal amount of matter and antimatter [3,4]. Baryogenesis, a dynamical mechanism, is required to explain the baryon asymmetry of the current universe (BAU) [5]. Understanding DM particles' nature, mass scale, and matter-antimatter asymmetry in the universe leads to new physics beyond the standard model (BSM). Observing neutrino masses [6] that arise from oscillation also suggests extending the SM. A new mechanism has been proposed [7,8] to simultaneously explain the DM abundance and BAU arising from B-meson oscillation that could be testable in B-factories, i.e., *BABAR* and Belle II experiments. The mechanism is suitable for low-scale baryogenesis and DM production. In the proposed model, baryogenesis occurs due to out-of-thermal equilibrium production of b and $\bar{b}$ quarks in the early universe through the decay of a massive, long-lived scalar field denoted as Φ, as shown in figure 1. The b quarks, injected into the universe at low temperature, will mostly hadronized as B mesons, e.g., B^0_d,B^0_s, and $B^{\pm}$. Upon hadronization the neutral B^0_q mesons will quickly undergo CP-violating oscillation before decaying into an SM baryon (p,Λ, etc.), a dark sector anti-baryon ψ_D, and any number of additional light meson $\mathcal{M}$. If the B mesons possess a non-standard decay channel into a dark sector anti-baryon ψ_D and an SM baryon; this result in the generation of a baryon asymmetry in the visible sector that is exactly compensated by a dark anti-baryon asymmetry. As a consequence, the total baryon number is actually conserved. A TeV mass-coloured, electrically charged scalar particle Y is introduced to generate effective interactions between the dark and visible sectors.

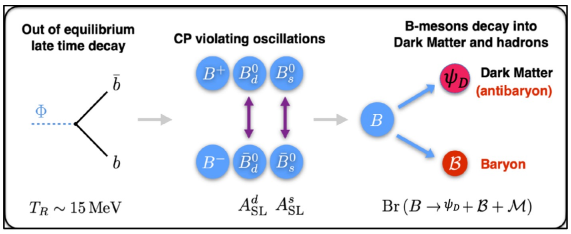

Figure 1: Summary of the Baryogenesis mechanism. Figure illustrated from references [7,8,9].

Analyses presented in this proceedings paper require one of the B mesons produced in $e^+e^- \to B^+B^-$ or $e^+e^- \to B^0\bar{B}^0$ is fully reconstructed from known hadronic decay modes, and we call it as B_{tag} [10], which is reconstructed via the decays $B \to SX$ explained in [11]. The rest of the event, denoted as B_{sig}, is the other B meson, which must include the SM baryon, e.g. proton, Λ, etc.

The *BABAR* detector, described elsewhere [12,13], is a general-purpose detector at the PEP-II asymmetric energy e^+e^- collider at the SLAC National Accelerator Laboratory. The detector was operated from 1999 to 2008 and collected data in Υ(4S, 3S, 2S) on and off resonances. In both analyses, we used $398.5 fb^{-1}$ [14] $\Upsilon(4S)$ data as signal events. About $32.5 fb^{-1}$ is used to optimize the analysis strategies, e.g. event selection and efficiencies measurement, which is then excluded from the sample used to obtain the final result. Simulated signal events are generated by using the event generator EVTGEN [15] in eight different masses ranging from 1 to 4.2 GeV/c^2. A combinatorial background, also known as continuum $e^+e^- \to q\bar{q}$ (q=udcs) along with the inclusive $B\bar{B}$ events are used as background and produced by Monte Carlo (MC) event generator, e.g. for $B\bar{B}$ events EVTGEN [15] is used whereas for $q\bar{q}$ JETSET [16,17] is used. The detector response for the MC events is simulated with GEANT4 [18].

2. Baryogenesis and Dark Matter in $B^+ \to \psi_D + p$ Decays

In this analysis, a B meson decays into a dark-sector antibaryon, denoted as ψ_D and an SM baryon proton (p) as shown in figure 2. The charge conjugation of that B meson decays into a dark-sector baryon, and an anti-proton is also considered. In other words, $B^+ \to \psi_D + p$ decays are selected in events in which a hadronic decay of B^- is fully reconstrcted. From kinematics perspective we see that $B \to \psi_D \mathcal{B}$ decay occur only if $m_{\psi_D} < m_B - m_p$ and for proton stability it requires $m_{\psi_D} > m_p - m_e$. Samples were made for eight different ψ_D mass hypotheses: 1.0, 1.5, 2.0, 2.5, 3.0, 3.5, 4.0, and 4.2 GeV/c^2. The dark-sector antibaryon ψ_D is identified as the system recoiling against the B_{tag} and the SM baryons. Two kinematic variables are considered to select B_{tag} candidates: beam-energy-substituted mass $m_{ES}c^2 = \sqrt{E_{beam}^2 - p_{B_{tag}}^2 c^2}$, where $p_{B_{tag}}$ is the three momentum of B_{tag} in the centre-of-mass (CM) frame; and the energy difference between the B_{tag} and the beam energy E_{beam}, i.e. $\Delta E = E_{beam} - E_{B_{tag}}$. E_{beam} is also in the CM frame and $E_{B_{tag}}$ must be within $\pm$ 0.2 GeV of the beam energy. We also require m_{ES} of the B_{tag} to lie within the nominal B^+ mass range as 5.27 - 5.29 GeV/c^2. For more than one B_{tag} candidates in an event, we choose the lowest ΔE related B as tagged B-meson.

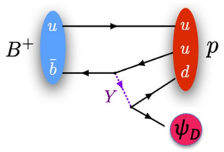

Figure 2: Figure taken and modified from [8].

On the signal side, we require one and only one track that is consistent with the proton mass. A multivariate selection using boosted decision trees (BDTs) [19] is used to suppress the remaining backgrounds in the signal that includes the following kinematics variables from the B_{tag}, i.e. m_{ES} and ΔE; information about the hadronic decay channel and its purity; and the magnitude of the thrust vector. The total extra neutral energy on the signal side in the CM frame, the cosine of the polar angle of the missing momentum vector recoiling against the B_{tag} meson and the signal candidates in the laboratory frame, the number of neutral particles and the number of π^0 candidates on the signal side are also included.

PoS(EPS-HEP2023)048

Figure 3a represents the distribution of the BDT response v_{BDT} for data, backgrounds, and eight simulated signal samples, and we select events with $v_{BDT} > 0.95$, which retains 99.97% of the simulated signal and 0.0028% of the simulated backgrounds. Figure 3b shows the distribution of m_{ES} for inclusive MC background, signal, and data. One can see that the signal events peak around the nominal B-meson mass, and background events are dominated by the continuum. Figure 3c represents the correction factors from discrepancies in the simulation of $B\bar{B}$ and $q\bar{q}$ events by using the ratio of the second-to-zeroth Fox-Wolfram moment [20] in two stages: $R_2 > 0.7$ for the $q\bar{q}$ correction factor $f_{q\bar{q}} = 1.05 \pm 0.03$; and $R_2 < 0.7$ for the $B\bar{B}$ correction factor $f_{B\bar{B}} = 0.85 \pm 0.07$.

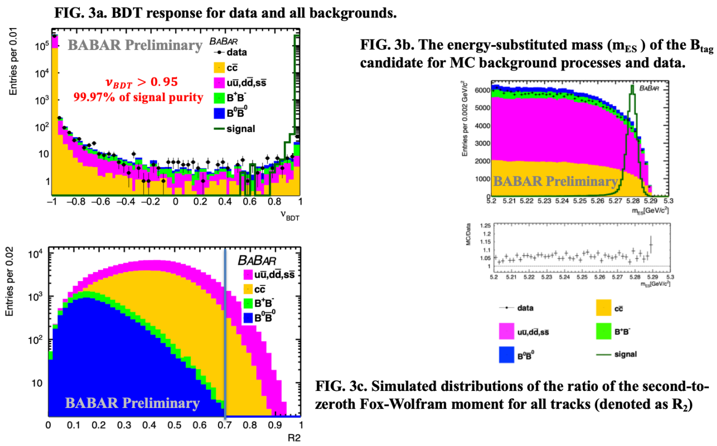

Figure 3: BDT response (3a), m_{ES} distributions (3b), and correction factors (3c) for data, signal, and backgrounds. Figures are taken from [21].

Signal efficiency varies from 0.00145 to 0.0006 for the eight simulated masses from ψ_D = 1.0 GeV/c^2 to $\psi_D = 4.2$ GeV/c^2. The missing mass m_{miss} as shown in figure 4, which in the case of a signal would be ψ_D mass, is calculated from the four momenta of the signal B_{sig} and proton: $m_{miss}c^2 = \sqrt{(E_{B_{sig}} - E_p)^2 - (\vec{p}_{B_{sig}} - \vec{p}_p)^2}$. For each signal mass, the m_{miss} distribution is fitted with a double-sided Crystal Ball function to extract the signal mass resolution. A total of 127 mass hypotheses with equal step size were considered in the range $1.0 < m_{miss} < 4.29$ GeV/c^2. The largest systematics come from the data/MC ratio and affect the signal efficiency is 8.4%. Other systematics are reported in the reference [21].

3. B mesogenesis

We also search for mesogenesis in $B^0 \to \psi_D + \Lambda$ [22] and its charge conjugate. We follow a similar procedure as $B^+ \to \psi_D +$ proton analysis in section 2. Here ψ_D identified against B_{tag} and SM baryon Λ. The candidate Λ is reconstructed as a pair of oppositely charged tracks identified as a proton and a pion.

Figure 5a represents the distribution of the energy-substituted mass m_{ES} for data, signal MC for $m_{\psi_D} = 2.0$ GeV/c^2 and inclusive background MC predictions. Figure 5b represents the reconstructed mass m_Λ distribution, whereas figure 5c represents the BDT score distribution respectively. We require events to satisfy $5.27 < m_{ES} < 5.29$ GeV/c^2

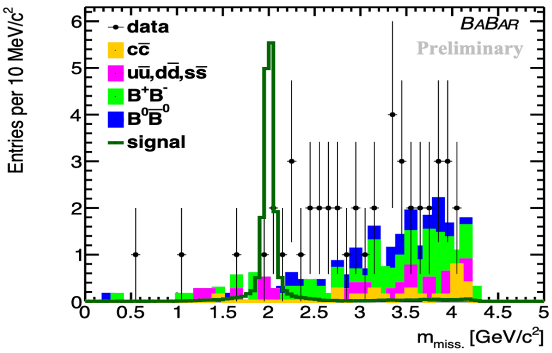

Figure 4: Missing-mass distributions after all selections are applied for a simulated signal sample [21].

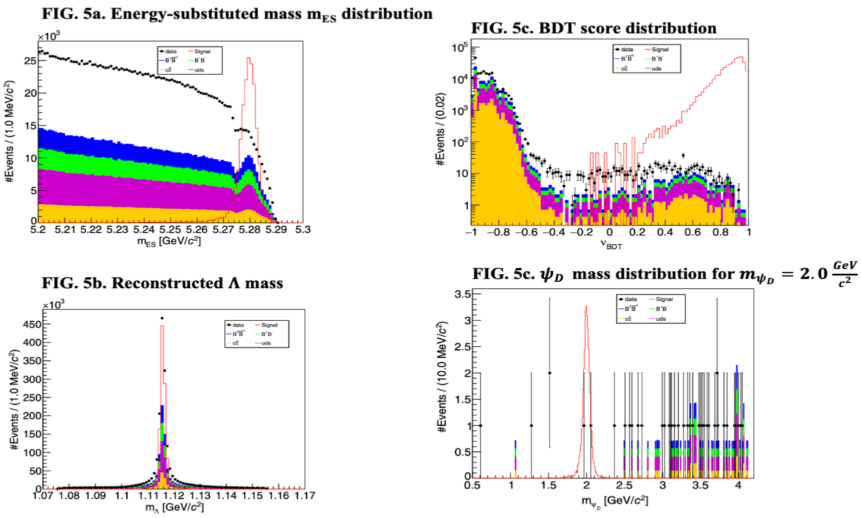

Figure 5: m_{ES}, m_Λ, BDT score, and missing-mass distributions after all selections are applied [22].

and $1.110 < m_\Lambda < 1.121\ GeV/c^2$. After all the selections are applied, the distribution of ψ_D mass m_{ψ_D} is plotted in figure 5d. Total systematic uncertainties arising from different sources in this analysis vary from 7.8% to 9.1% [22].

4. Conclusion

No significant signal was observed, and due to the absence of a signal, 90% confidence level (C.L.) upper limits on the branching fraction are derived in both analyses [21,22] using a profile likelihood method [23]. Results from $B^+ \to \psi_D + p$ constraints the branching fraction upper limit on R-Parity violation coupling [21]. These results exclude a significant fraction of the parameters space explained in [7,8] that are allowed by B mesogenesis. Future measurements at Belle-II should be able to explore the remaining region fully.

PoS(EPS-HEP2023)048

References

[1] Planck Collaboration, P. A. R. Ade et al, Planck 2015 results, Astronomy and Astrophysics 594, A13 (2016).

[2] Planck Collaboration, N. Aghanim et al., Planck 2015 results, Astronomy and Astrophysics 641, A6 (2020).

[3] E. W. Kolb and M. S. Turner, The Early Universe, Front. Phys. 69, 1 (1990).

[4] V. A. Rubakov and D. S. Gorbunov, Introduction to the Theory of the Early Universe: Hot Big Bang Theory, World Scientific, Singapore, 2017.

[5] L. Canetti, M. Drewes, and M. Shaposhnikov, Matter and antimatter in the universe, New Journal of Physics 14, 095012 (2012).

[6] SNO Collaboration, Q. R. Ahmad et al., Direct Evidence for Neutrino Flavor Transformation from Neutral-Current Interactions in the Sudbury Neutrino Observatory, Phys. Rev. Lett. 89, 011301 (2002).

[7] G. Elor, M. Escudero, and A. E. Nelson, Baryogenesis and dark matter from B mesons, Phys. Rev. D 99, 035031 (2019).

[8] G. Alonso-Alvarez, G. Elor, and M. Escudero, Collider signals of baryogenesis and dark matter from B mesons: A roadmap to discovery, Phys. Rev. D 104, 035028 (2021).

[9] BABAR Collaboration, J. P. LEES et al., Search for B mesogenesis at BABAR, PHYS. REV. D 107, 092001 (2023).

[10] BABAR, BELLE Collaborations, A. J. Bevan et al., The Physics of the B Factories, Eur. Phys. J. C 74, 3026 (2014).

[11] BABAR Collaboration, J. P. Lees et al., Search for $B^- \to \Lambda\bar{p}\nu\bar{\nu}$ with the BaBar experiment, Phys. Rev. D 100, 111101 (2019).

[12] BABAR Collaboration, B. Aubert et al., The BABAR Detector, Nucl. Instrum. Methods Phys. Res., Sect. A 479, 1 (2002).

[13] BABAR Collaboration, B. Aubert et al., The BaBar detector: Upgrades, operation and performance, Nucl. Instrum. Methods Phys. Res., Sect. A 729, 615 (2013).

[14] BABAR Collaboration, J. P. Lees et al., Time-integrated luminosity recorded by the BABAR detector at the PEP-II e^+e^- collider, Nucl. Instrum. Meth. A 726, 203 (2013).

[15] D. J. Lange, The EvtGen particle decay simulation package, Nucl. Instrum. Meth. A 462, 152 (2001).

[16] T. Sjostrand, High-energy-physics event generation with PYTHIA 5.7 and JETSET 7.4, Comp. Phys. Commu. 39, 347 (1986).

[17] T. Sjostrand and M. Bengtsson, The Lund Monte Carlo for jet fragmentation and e^+e^- physics-jetset version 6.3-an update, Comp. Phys. Commu. 43, 367 (1987).

[18] S. Agostinelli et al. (GEANT4), Geant4—a simulation toolkit, Nucl. Instrum. Meth. A 506, 250 (2003).

[19] Y. Freund and R. E. Schapire, A Decision-Theoretic Generalization of On-Line Learning and an Application to Boosting, J. Comput. Syst. Sci. 55, 119 (1997).

[20] G. C. Fox and S. Wolfram, Observables for the Analysis of Event Shapes in e^+e^- Annihilation and Other Processes, Phys. Rev. Lett. 41, 1581 (1978).

[21] BABAR Collaboration, J. P. Lees et al.,Search for Baryogenesis and Dark Matter in $B^+ \to \psi_D + p$ Decays at BABAR, arXiv:2306.08490v3.

[22] BABAR Collaboration, J. P. Lees et al., Search for B mesogenesis at BABAR, Phys. Rev. D 107, 092001 (2023) .

[23] W. A. Rolke, A. M. Lopez, and J. Conrad, Limits and Confidence Intervals in the Presence of Nuisance Parameters, Nucl. Instrum. and Meth. A 551, 493 (2005).

PoS(EPS-HEP2023)048